Available online at www.sciencedirect.com
ScienceDirect
International Journal of Heat and Mass Transfer 50 (2007) 5177–5193
International Journal of HEAT and MASS TRANSFER
www.elsevier.com/locate/ijhmt

Examination of heat transfer correlations and a model for flow boiling of R134a in small diameter tubes

D. Shiferaw [a], X. Huo [b], T.G. Karayiannis [a,*], D.B.R. Kenning [a]

[a] Brunel University, School of Engineering and Design, Uxbridge UB8 3PH, UK
[b] Oaksmere Refrigeration Design and Consultancy, Stowmarket, UK

Received 27 March 2007; received in revised form 3 July 2007
Available online 13 August 2007

Abstract

Analysis of various existing correlations including a three-zone evaporation model is made using a comparison with recent experimental results obtained in this study. Flow boiling heat transfer experiments were conducted with two stainless steel tubes of internal diameter 4.26 mm and 2.01 mm. The working fluid was R134a and parameters were varied in the range: mass flux 100–500 kg/m^{2}s; pressure 8–12 bar; quality up to 0.9; heat flux 13–150 kW/m^2. The local heat transfer coefficient was independent of vapour quality when this was less than about 40–50% in the 4.26 mm tube and 20–30% in the 2.01 mm tube. Local transient dryout was deduced when the quality was above these values. Furthermore, at high heat flux values the heat transfer coefficient decreased with vapour quality for the entire quality range indicating early occurrence of dryout.

Existing correlations, which are based on large tube boiling processes, do not predict the present small diameter data to a satisfactory degree. A better agreement is observed with the recent, state-of-the-art, three-zone evaporation model. However, the model does not predict the effect of diameter and the partial dryout. Nevertheless, the observation suggests that the flow pattern based modelling approach performs at least as well as empirical correlations that are based on macroscale modelling. Aspects of the model that need further consideration are also proposed in this study.

Keywords: Flow boiling; Flow pattern; Heat transfer; Two-phase flow; Small diameter

1. Introduction

Flow boiling heat transfer in small diameter tubes and microchannels is a subject of intense research. Despite the fact that various heat transfer correlations have been proposed, many of them empirically formulated from a rigorous data analysis, hydrodynamic and thermal aspects of boiling in small diameter tubes are not well understood. Moreover, there are only a few theoretical models that link the heat transfer mechanism with flow regimes observed in small diameter tubes. This paper compares experimental data for R134a boiling in 4.26 and 2.01 mm tubes at pressures of 8–12 bar with correlations for flow boiling in small tubes and with the three-zone evaporation model of Thome et al. [1] for the slug flow regime.

There is no clear definition of the classification criterion for the size range in small/mini/microchannel two-phase flow study. Most of the ways used to classify the various size ranges do not consider the physical mechanism and other effects involved when varying the size of the channels. Some definitions of microscale hydraulic diameter classification are suggested in the literature. Kandlikar and Grande [2] recommended: conventional channels ($d_h \geqslant 3$ mm), minichannels (200 μm $\leqslant d_h < 3$ mm) and microchannels (10 μm $\leqslant d_h < 200$ μm). The surface tension forces influence the mechanism of heat transfer in small tubes; as the diameter of the tube decreases, the surface tension force surpasses the effect of gravity. Only a few attempts have been made to address these issues in the classification

* Corresponding author.
E-mail address: tassos.karayiannis@brunel.ac.uk (T.G. Karayiannis).

0017-9310/$ - see front matter © 2007 Elsevier Ltd. All rights reserved.
doi:10.1016/j.ijheatmasstransfer.2007.07.002

Nomenclature

Bo	Bond number, $g(\rho_l - \rho_v)d^2/\sigma$
Co	Confinement number, $[\sigma/g(\rho_l - \rho_v)]^{1/2}/d$
$C_{\delta 0}$	correcting factor on the initial film thickness
d	diameter (m)
f	pair frequency (Hz)
G	mass flux (kg m^{-2} s^{-1})
g	gravitational acceleration (m s^{-2})
h	enthalpy (J kg^{-1})
h_{lv}	latent heat of vaporization (J kg^{-1})
L	length (m)
m	mass flow rate (kg s^{-1})
Nu	Nusselt number, $\alpha d_h/\lambda$
P	pressure (Pa)
Q	heat (W)
q	heat flux (W m^{-2})
Re	Reynolds number, Gd_h/μ
T	temperature (K)
t	time (s)
U	velocity (m s^{-1})
We	Weber number, $G^2 d_h/\rho_l \cdot \sigma$
X	Martinelli parameter, $(G_l/G_v)^{0.9}$ $(\rho_v/\rho_l)^{0.5}(\mu_l/\mu_v)^{0.1}$
x	thermodynamic quality
z	axial distance (m)

Greek symbols

α	heat transfer coefficient (W m^{-2} K^{-1})
Δ	finite increment
δ	liquid film thickness (m)
λ	thermal conductivity (W m^{-1} K^{-1})
v	kinematic viscosity (m^2 s^{-1})
ρ	density (kg m^{-3})
σ	surface tension (N m^{-1})
τ	pair period (s)

Subscripts

crit	critical
dry	dryout zone
end	end
film	liquid film between bubble and wall
h	hydraulic
i	index
l	liquid
lo	liquid only
min	minimum
opt	optimum
p	pair
ref	reference
tp	two-phase
tt	liquid-turbulent and gas-turbulent
v	vapour
w	wall
0	initial

theory. Kew and Cornwell [3] examined the effects of geometry and size on two-phase flow and heat transfer. They defined the threshold criterion where macroscale heat transfer modelling becomes unreliable for predicting flow boiling heat transfer coefficients as a function of the confinement number. This is the square root of the reciprocal of the Bond number, which is the ratio of the gravity and surface tension forces so, $Co = [\sigma/g(\rho_l - \rho_v)]^{1/2}/d$. As the diameter decreases or the Co number increases above the threshold given by this criterion, i.e. $Co = 0.5$ ($Bo = 4$), bubble growth is assumed to be confined by the channel to the point where individual bubbles grow in length rather than in diameter. This is variously termed the elongated bubble regime, confined bubble flow or (following macro channel terminology) slug flow. Recently, Chen et al. [4] examined the flow patterns at qualities $x > 0$ leaving tubular boiling test sections ranging in diameter from 4.26 mm down to 1.1 mm for R134a over the pressure range 6–14 bar. The flow patterns were observed by digital high-speed camera in a borosilicate glass tube with an internal diameter matched to the test section and installed at its exit, providing an adiabatic length for flow development. Chen et al. [4] defined the conventional regimes of dispersed bubble, bubbly, slug, churn, annular and annular-mist flow. In addition, they departed from the above terminology by distinguishing slug flow (bullet shaped bubbles with sharp corners and a fluctuating surface at the rear) from confined bubble flow (bubbles with convex rear ends). Confined bubble flow occurred for a combination of low liquid and vapour superficial velocities. It was observed in the 2.01 mm tube only at the lowest pressure of 6 bar but occurred at all pressures in the 1.10 mm tube. For these same combinations of pressure and diameter, the liquid–vapour interfaces in slug and churn flow that occurred at higher liquid and vapour velocities were less disturbed. These indications of the increasing importance of surface tension with decreasing diameter were consistent with the diameters predicted by the confinement number criterion, which for R134a ranged from 1.7 mm at 6 bar to 1.4 mm at 14 bar. There is no particular reason why there should be a sharp threshold for the onset of the influence of surface tension, nor is it obvious that the controlling factor should be the ratio of surface tension forces to hydrostatic forces rather than hydrodynamic forces. Flow regimes may also transform gradually, rather than have sharp boundaries. Chen et al. [4] determined the regime boundaries (corresponding to the midpoint of a transition zone) by visual analysis of video recordings at fixed total mass flow for increasing vapour flow created by small increments in the heat input to the test section, using criteria defined in

their paper. While further tests over a wider range of conditions may be required to determine whether it is indeed necessary to plot a boundary between confined bubble and slug flow, they found that the boundaries between the other regimes could be determined with sufficient consistency to identify the influences of pressure and tube diameter. Examples of dimensional regime maps from [4] for different diameters at pressures of 6 and 14 bar using the superficial velocities of the liquid and vapour phases as coordinates are shown in Fig. 1, excluding the confined bubble–slug flow boundary. Constant mass flux and constant quality lines are superimposed on the maps in Chen's

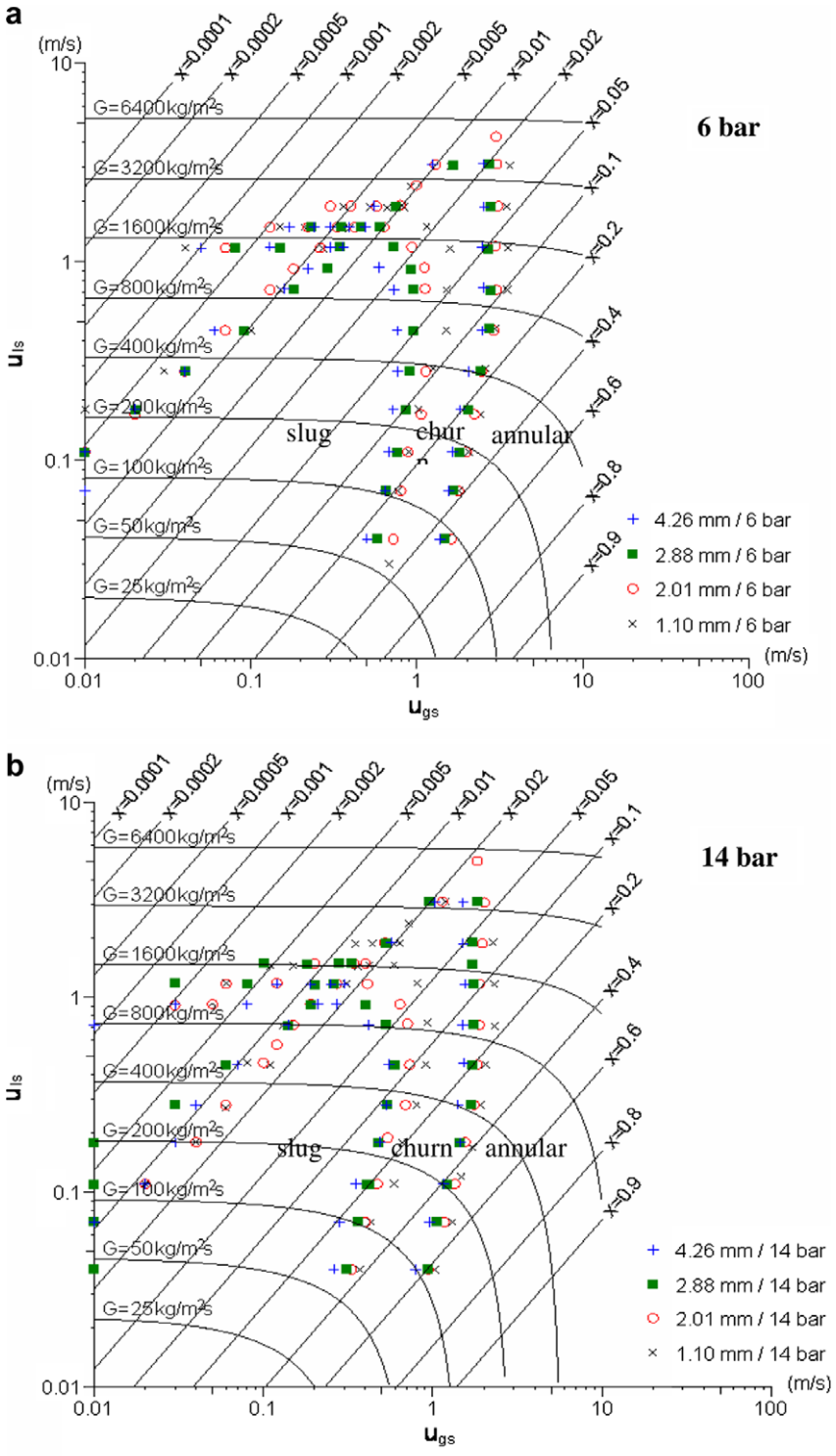

Fig. 1. Flow regime boundaries for R134a in tubes of diameter 1.10–4.26 mm. Dimensional plot of U_{ls} vs. U_{gs} with constant mass flux and quality lines at: (a) 6 bar (b) 14 bar, Chen [5].

thesis, [5]. The maps for different diameters collapsed onto a single map in a non-dimensional plot employing the liquid and vapour Weber numbers (the ratio of surface tension forces to hydrodynamic forces). With increasing pressure, the regime boundaries shifted to slightly higher vapour Weber numbers, [4]. Chen et al. [4] suggested this as a tentative method of predicting flow regimes, noting that further work was required including the examination of the uncertainty in the width of the transition zones between regimes. Any regime map that uses local flow parameters as coordinates assumes that flow regimes are not affected by the heat flux and the local fluctuations that become stronger with decreasing diameter in the boiling section, nor by flow development in the adiabatic observation section. Explicit information about flow regime boundaries is rarely required for heat transfer correlations but it is necessary to define the range of validity of mechanistic models that are regime-specific. The maps in Chen et al. [4] have been used for this purpose in this paper when comparing experimental data for R134a with the Thome et al. [1] model for the slug flow regime.

There are limited experimental works that have investigated the effect of diameter by testing a wide range of passages of various diameters. Some researchers including Yan and Lin [6], Agostini and Bontemps [7], Palm [8] and Huo [9] have experimentally showed that the heat transfer coefficient increases when the diameter decreases. Various experimental results from different research groups have shown discrepancies regarding the effect of other parameters such as vapour quality, mass flux, heat flux and saturation pressure on the heat transfer coefficient. Based on the results, various interpretations have been given for the heat transfer mechanism in small diameter tubes such as: forced convection, nucleate boiling, transient film evaporation surrounding the confined bubbles, convection and evaporation of the wavy annular film. A number of researchers including Lazarek and Black [10], Wambsganss et al. [11], Tran et al. [12], Bao et al. [13] and Huo et al. [14], experimentally demonstrated that the heat transfer coefficient is nearly independent of vapour quality and mass flux, while it is strongly dependent on heat flux and saturation pressure. Conventionally, this is interpreted as evidence that nucleate boiling is the dominant heat transfer mechanism. A small number of researchers, e.g. Carey et al. [15] said that nucleation was not an important mechanism because, in their experiments, heat transfer coefficients were independent of heat flux, dependent on mass flux, and increased with quality.

A number of researchers have studied the fluctuations in pressure and wall temperature but few have analysed the confined bubble using local measurements synchronised with a video of the bubble motion. Yan and Kenning [16] investigated water boiling at atmospheric pressure in a 2×1 mm channel. They showed that the pressure fluctuations were caused by the acceleration of liquid slugs by expanding confined bubbles, confirming a model of Kew and Cornwell [17], and that the corresponding fluctuations in saturation temperature were of similar magnitude to the mean superheat causing evaporation, so they could not be neglected. The fluctuations were accompanied by cyclic changes in the local mechanism of heat transfer between single and two-phase convection and nucleate boiling that did not fit the conventional interpretations of time-averaged heat transfer coefficients, Kenning and Yan [18], Wen et al. [19]. Brutin and Tadrist [20] made similar local observations for *n*-pentane boiling in a 4×1 mm channel and observed that the average heat transfer coefficient reached its peak value in the fluctuating regime.

The bubbles in small diameter tubes grow rapidly to confined bubbles which ultimately fill the tube. Consequently there is sometimes a direct transition from confined bubble to annular flow under certain conditions. At high heat flux, the rapid expansion of bubbles expels the liquid, creating an intermittent local dryout, until the next liquid is replenished. Zhang et al. [21,22] noted that the highest heat transfer in their microchannels was achieved in confined bubble flow at sufficiently low time-averaged exit quality to avoid dryout of the liquid film round the bubbles. Wen et al. [23] observed at very low mass fluxes the downstream propagation of transient high wall temperatures indicative of dryout, even at low heat fluxes. In channels of circular cross-section, in which events in the boiling region cannot be observed directly, decreases in time-averaged heat transfer coefficient with increasing quality, often accompanied by fluctuating wall temperatures, have been attributed to transient dryout, particularly at low mass flux, [9]. There have been few studies that investigated the mechanism of dryout in small channels. Kenning et al. [24] suggested that there are two different mechanisms of dryout around individual bubbles in microchannels. These are dryout as a result of depletion of the film thickness below a certain minimum by complete evaporation of the liquid film beneath the confined bubble and dry out due to surface tension driven 'capillary roll-up' on partially-wetted surfaces with finite contact angles.

There may be two different sorts of partial dryout in the slug flow regime in small tubes. One is a cyclical process caused by regular dryout of the liquid film near the rear of each confined bubble, analogous to dryout of the microlayer under individual bubbles in pool nucleate boiling. The other may involve several bubbles or the expulsion of liquid from the tube, so that it has a longer timescale and is analogous to transition boiling preceding film boiling in pool boiling. Microchannel heat transfer correlations generally do not consider either type of partial dryout and there are no correlations or models that predict the effects of the second type of dryout on heat transfer and the vapour quality at which it occurs.

Various recent flow boiling correlations, along with a more detailed presentation of the three – zone evaporation model proposed by Thome et al. [1] (which does include the first type of cyclic dryout), are briefly introduced in Section 2 of this paper. The correlations and the model are then compared with experimental results obtained with two

stainless steel tubes of internal diameter 4.26 mm and 2.0 mm, using R134a at 8 bar and 12 bar system pressures.

2. Brief summary of some recent correlations and a model

Only recent correlations and a model are discussed here. The comparison with the Lazarek and Black [10], Gungor and Winterton [25] and Tran et al. [12] correlations were first presented in Huo et al. [14]. Table 1 summarises briefly the conclusions of the comparison for 8 and 12 bar.

Kandlikar [26] modified the Kandlikar [27] correlation, which was developed to predict saturated flow boiling heat transfer coefficients for large diameter tubes of high Reynolds number based on the single-phase, all-liquid, heat transfer coefficient. It was based on a model utilizing the contributions of nucleate boiling or convective mechanisms by taking the greater of the two. The main developments in the recent correlation include the extension of the single-phase all-liquid heat transfer coefficient to the laminar region and considering no convective boiling contribution for deep laminar regions. The correlations which were used for the single-phase all liquid heat transfer coefficient can be summarized based on the different regimes as follows: the Gnielnski [28] and Petukhov and Popov [29] correlation were used for the turbulent region ($Re_{lo} \geqslant 3000$); $Nu = 4.36$ was used for the laminar region ($Re_{lo} < 1600$). For the transition region ($1600 \leqslant Re_{lo} < 3000$), linear interpolation of the heat transfer coefficient between laminar and turbulent flow was used. The convective boiling contribution was neglected for the deep laminar region ($Re_{lo} \leqslant 100$).

The original Chen [30] correlation was developed for liquid-turbulent and gas-turbulent flow conditions, so the Martinelli parameter $X = X_{tt}$. Following on from that, Zhang et al. [31] extended the correlation to the liquid-laminar and gas-turbulent conditions considered to characterise boiling in mini-channels by introducing a factor dependent on the Reynolds number. For the single-phase heat transfer coefficient the Dittus–Boelter correlation was used for the turbulent region ($Re_{lo} > 2300$); $Nu = 4.36$ for the laminar region ($Re_{lo} < 2000$) and linear interpolation was used between laminar and turbulent for the transition region ($2000 < Re_{lo} < 2300$).

It can be seen from the above that Kandlikar [27] and Zhang et al. [31] have a different classification threshold for the laminar and turbulent regions. This is one of the issues that are not clearly defined in microchannel two-phase flow studies.

2.1. The three-zone evaporation model [1]

The model predicts the local dynamic and the local time-averaged heat transfer coefficient at fixed locations along the channel based on the evaporation of elongated bubbles. Following the passage of a liquid slug, a bubble is modelled to pass as a confined elongated bubble trapping a thin liquid film against the inner wall. If the liquid film dries out before the arrival of the next liquid slug, then a vapour slug follows (triplet). If not, then the model assumes the existence of a pair consisting of the liquid slug and the elongated bubble. Therefore, a novel feature of the model is that it considers a dryout zone and exploits the transient evaporation of the film. The model does not include a contribution from nucleate boiling.

For the purpose of the present comparisons, it is necessary to summarise the model briefly, in order to highlight important and relevant parameters that will be discussed later. The local heat transfer coefficient is given as the time averaged of the three zones: (1) liquid slug, (2) elongated bubble and (3) dryout zone.

$$\alpha_{tp}(z) = \frac{t_l}{\tau}\alpha_l(z) + \frac{t_{film}}{\tau}\alpha_{film}(z) + \frac{t_{dry}}{\tau}\alpha_v(z) \quad (1)$$

where

$$\tau = \frac{1}{f} \quad (2)$$

The mean heat transfer coefficient through the evaporating thin liquid film surrounding the elongated bubble, was obtained by assuming one–dimensional heat conduction in a

Table 1
Summary of the prediction results of the existing correlations for the present data, [14]

Authors [Reference]	Channel size and geometry	Fluid and parameter range	Comparison results of [14]
Lazarek and Black [10]	3.15 mm, single tube	R113 $G = 125$–750 kg/m^2 s $P = 1.3$–4.1 bar $q = 14$–380 kW/m^2	Under-predicted the experimental results of 4.26 and 2.01 mm at pressure of 8 and 12 bar by about 30% or more. The disagreement increased with pressure.
Gungor and Winterton [26]	3.0–32 mm,	R11, water $G = 12.4$–61518 kg/m^2 s $P = 0.08$–202.6 bar $q = 0.35$–91×10^3 kW/m^2	Under-predicted the experimental results by 30% for the 4.26 mm at 8 bar and by more than 30% at 12 bar. Relatively less under-prediction, within 25% was obtained for the 2.01 mm at 8 bar.
Tran et al. [12]	2.46 mm, single tube 4.06×1.7 mm, single rectangular channel	R12 $G = 44$–832 kg/m^2 s $P = 5$–8 bar $q = 3.6$–129 kW/m^2	Consistently under-predicted the 4.26 mm data within 30%. The prediction was worse for the 2.01 mm tube. There was no pressure effect in the comparison for both tubes

stagnant thin liquid film. This assumption may mean that the model should not be applied in the unstable conditions of churn flow, in which conduction may be enhanced.

The researchers did not define three parameters by fundamental analysis, namely the minimum thickness of the liquid film at dryout (δ_{min}), the pair frequency (f), which is the frequency of the bubble generation and the correction factor, $C_{\delta 0}$ for initial film thickness. These parameters had to be found by optimising the prediction of the model against an experimental database for the heat transfer coefficient. The initial thickness of the liquid film was found by using the Moriyama and Inoue [32] film thickness prediction and applying an empirical correction factor, $C_{\delta 0}$ as shown in Eq. (3). Dupont et al. [33] compared the model predictions with a database (1591 test data for R11, R12, R113, R123, R134a, R141b and CO_2) and recommended general values of the parameters after optimising empirically each parameter with the whole range of the database.

$$\frac{\delta_0}{d} = C_{\delta_0}\left(3\sqrt{\frac{\nu_l}{U_p d}}\right)^{0.84}\left[(0.07Bo^{0.41})^{-8} + 0.1^{-8}\right]^{-1/8} \tag{3}$$

$$\delta_{min} = 0.3\ \mu m \tag{4}$$

$$f_{opt} = \left(\frac{q}{q_{ref}}\right)^{1.74} \text{Hz} \tag{5}$$

$$q_{ref} = 3328\left(\frac{P_{sat}}{P_{crit}}\right)^{-0.5} \tag{6}$$

$$C_{\delta 0} = 0.29 \tag{7}$$

In the current paper, the above recommended values of the three parameters were used in the comparison with the experimental result. It is desirable, however, to obtain independent estimates of the three parameters from detailed observations.

An experimental facility was used to determine the heat transfer coefficient in small diameter tubes using R134a fluid. The experimental method is described in Section 3. Some of the heat transfers results and the comparisons with existing recent correlations and with the model of Thome et al. [1] will be presented in Sections 4 and 5, respectively.

3. Experimental facility and procedure

The experimental facility was described in detail in Huo et al. [9,14]. The test sections were made of stainless steel cold drawn tubes; the first one was 4.26 mm in internal diameter, internal roughness 1.75 μm with 0.245 mm wall thickness and 500 mm in length; the second test tube was 2.01 mm in internal diameter, roughness 1.82 μm with 0.19 mm wall thickness and 211 mm in length. A borosilicate glass tube for flow pattern observation was located immediately downstream of the heat transfer test section. A digital high-speed camera (Phantom V4 B/W, 512 × 512 pixels resolution, 1000 pictures/s with full resolution and maximum 32,000 pictures/s with reduced resolution, 10 μs exposure time) was used to observe the flow patterns.

All the instruments were carefully calibrated. The uncertainty in temperature measurement was ±0.16 K, flow rate measurements ±0.4%, and pressure measurements ±0.15%, [14]. The average error in the heat transfer coefficient was ±6%. A validation was performed using single-phase pressure drop and heat transfer tests before running the boiling experiment. The single-phase friction factor results agreed well with the Blasius correlation, i.e. within the uncertainty of the experiment. Also, the single-phase Nusselt number (Nu) results agreed very well with Dittus-Boetler and Petukhov correlation; again below the uncertainty limit. A series of flow boiling tests were then performed at different mass flux and heat flux. During these tests, the inlet temperature was controlled by adjusting the capacity of the chiller and heating power to the preheater. The flow rate was set to the required value and the heat flux was increased gradually until the exit quality reached about 90%. The data were recorded after the system was steady, which normally took about 15 min but sometimes longer. Each recording was the average of 20 measurements. The next test was then performed at a different flow rate.

The local heat transfer coefficient at each thermocouple point was determined based on the following equation:

$$\alpha = \frac{q}{T_w - T_l} \tag{8}$$

where T_w is the local inner wall temperature, T_l is the local fluid temperature and q is the inner wall heat flux to the fluid. T_l was deduced from the fluid pressure, which was determined based on the assumption of a linear pressure drop through the test section. T_w was calculated based on the outside surface temperature recorded by the thermocouples, heat flux and the tube wall thermal resistance. The heat lost to the ambient, ΔQ, was included in the calculation. It was obtained from single-phase experiments, [9,14]. An energy balance based on the heat supplied minus losses and the enthalpy change enabled the exit thermodynamic quality to be calculated. The total enthalpy change across the test section was calculated based on the flow rate of the refrigerant and the pressure and temperature change measured by the differential pressure transducer and thermocouple, respectively, at two ends of the test section. The thermodynamic quality (x) was determined based on the heat transferred to the fluid, given as

$$x_i = \frac{h_i - h_l}{h_{lv}} \tag{9}$$

where h_l and h_v are the specific enthalpy of saturated liquid and vapour, respectively. h_i is the local specific enthalpy of the fluid. This was determined from the enthalpy of the previous section and the heat transferred to the fluid, i.e.

$$h_i = h_{i-1} + \frac{L_i}{mL}(Q - \Delta Q) \tag{10}$$

where the heat input (Q) is equal to the product of the voltage and the current applied directly to the test section.

Local flow boiling heat transfer coefficients and flow patterns for R134a were obtained for the range: pressure 8 and 12 bar, heat flux 13–150 kW/m^2, mass flux 100–500 kg/m^{2}s, thermodynamic quality 0–0.9 and tube diameter 2.01 and 4.26 mm. The boiling experiments were performed over a period of 6 months and the long-term repeatability was the same as the short-term experimental uncertainty.

4. Experimental results

Typical experimental data for the local heat transfer coefficient are plotted in Fig. 2 as a function of quality at different heat fluxes for a pressure of 8 bar at a constant mass flux of 300 kg/m^{2}s in the 4.26 and 2.01 mm tubes. The flow pattern transition boundaries predicted by the Chen et al. [4] regime maps are also shown.

For the 4.26 mm tube, Fig. 2a, at qualities $x \leqslant 0.5$ approximately the heat transfer coefficient is constant within ±10% at a value that increases with increasing heat flux. Within this region, there is a pattern of small changes that become more pronounced with increasing heat flux: there is a small decrease from the first to the second measuring point, then an increase to a maximum value at the fifth measuring point, followed by a gradual decrease. Consequently, these features occur at higher values of x as the heat flux increases. They exceed the experimental uncertainty and do not occur in the single-phase tests, so they are though to be genuine and not the consequence of systematic errors at individual thermocouples. They do not appear to coincide with the flow regime boundaries deduced from [4]. For qualities >0.5, achievable only at the three heat fluxes $\geqslant$ 80 kW/m^2 and lying well in the annular flow regime according to [4], the heat transfer coefficient decreases rapidly with increasing quality and the data for the three high heat fluxes converge on a single line. The pattern of separate lines of nearly constant heat transfer coefficient at low quality merging with a single line of *increasing* heat transfer coefficient at higher quality is familiar in flow boiling experiments in large tubes performed with axially uniform heat flux and leads to the conventional interpretation of nucleate boiling at low quality

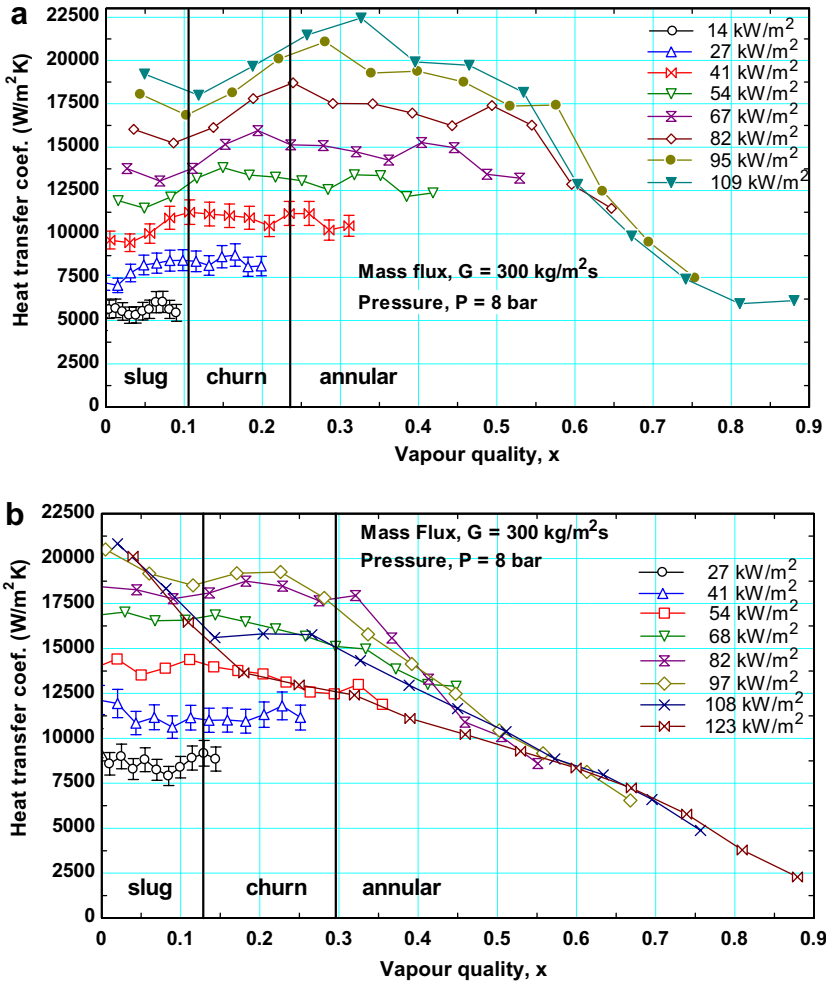

Fig. 2. Local heat transfer coefficient as a function of vapour quality with different heat fluxes; $G = 300$ kg/m^2 s, $P = 8$ bar. (a) $d = 4.26$ mm (b) $d = 2.01$ mm.

being suppressed as the wall superheat is depressed by the increase in convective heat transfer at high quality. This interpretation is inconsistent with the *decreasing* heat transfer coefficient and increasing wall superheat in the present experiments. In this particular region only, the tube wall temperature was observed to be highly unstable, leading to large fluctuations so that the experiment had to be stopped occasionally to avoid damaging the test section. It is therefore likely that the decrease in the heat transfer coefficient with increasing vapour quality may be attributable to the occurrence of partial (intermittent) dryout with a long timescale. The data logging system was not set up to record accurately rapid changes in wall temperature in these experiments and the nature of the variations will require further investigation.

The experimental data for the 2.01 mm tube at the same mass flux and system pressure, shown in Fig. 2b, exhibit similar characteristics of separate lines for each heat flux at low quality, merging into a single line of decreasing heat transfer coefficient with increasing quality in the tests at higher heat fluxes. The transition to decreasing heat transfer coefficient occurs at lower quality than in the 4.26 mm tube. At 68 kW/m^2, there is a gradual transition. At 82 kW/m^2, a sharper transition occurs at $x = 0.35$, just beyond the churn-annular boundary predicted by [4]. At 97 kW/m^2, it occurs at $x = 0.22$ in the churn flow region. For the two highest heat fluxes of 108 kW/m^2 and 123 kW/m^2, the region of decreasing heat transfer coefficient commences very close to the start of the heated length in the slug flow regime. The lines for the two heat fluxes coincide as far as the estimated slug-churn boundary, where there is a relative increase in the heat transfer coefficient for 108 kW/m^2 that persists until the lines for all heat fluxes merge in the annular regime.

The influence of system pressure on the heat transfer coefficient is illustrated in Fig. 3 for the 4.26 and 2.01 mm tubes for the same mass flux of 300 kg/m^{2}s and a nominal heat flux of 80 kW/m^2. (The actual heat flux

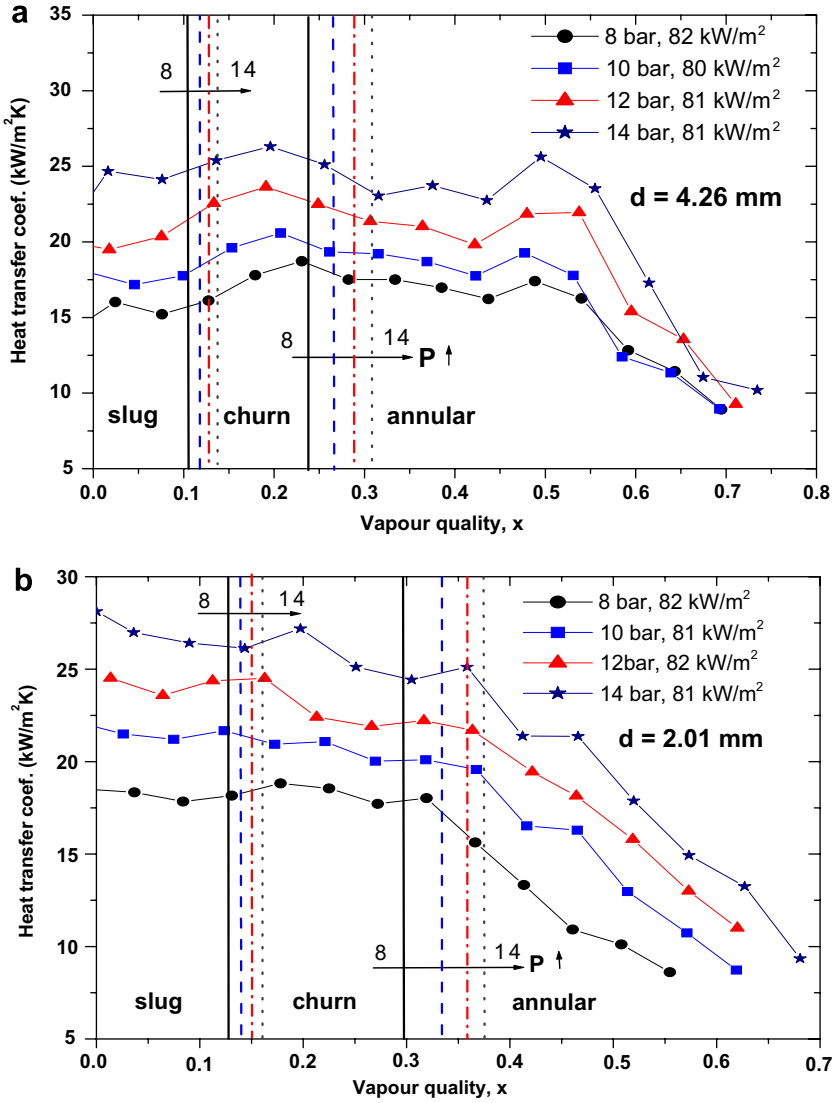

Fig. 3. Local heat transfer coefficient as a function of vapour quality for various system pressures, $G = 300$ kg/m^2 s, nominal $q = 80$ kW/m^2: (a) $d = 4.26$ mm (b) $d = 2.01$ mm.

for each run is shown on the graphs). The flow pattern transition boundaries from [4] shift to higher values of x with increasing pressure, the shift being slightly larger in the smaller tube. In the 4.26 mm tube, the approximately uniform heat transfer coefficients in the region $x \leqslant 0.5$ increase with system pressure. The dotted lines demonstrate the effect (shift) due to changes in system pressure. There is no change in the quality at which the transition to heat transfer coefficient decreasing with quality occurs. In this region, the effect of pressure becomes less regular and the heat transfer coefficient converges on 8–10 kW/m^2 at $x = 0.7$ for all pressures. In the 2.01 mm tube, there is a general increase in heat transfer coefficient with increasing pressure throughout the experimental range of quality. In the region of nominally constant heat transfer coefficient at low x, there is a slight decrease in the coefficient with increasing x at the higher pressures.

The dependence of the heat transfer coefficient on mass flux in the range 200–500 kg/m^2 s at 8 bar is investigated in Fig. 4 for the 4.26 mm and 2.01 mm tubes at nominal heat fluxes of 68 kW/m^2 and 80 kW/m^2, respectively. The flow regime boundaries based on [4] are shifted to significantly lower qualities as the mass flux increases (shown by the dotted lines). At low qualities, the approximately uniform values of the heat transfer coefficient are almost independent of the mass flux within experimental uncertainty for both tubes. The influence of mass flux on the transition to heat transfer coefficients that decrease with increasing quality is less clear. In the 4.26 mm tube, the transition occurs in the annular flow regime. The data for mass fluxes of 200 and 300 kg/m^2 s follow the same line throughout the range of measurement. Identifying the transition at the higher mass fluxes of 400 and 500 kg/m^2 s depends on the reliability of the decrease in heat transfer coefficient recorded at the last measuring station, which indicates a shift of the transition point to lower quality with increasing mass flux. In the 2.01 mm tube, the transition occurs in the nominal churn flow regime. The data for 200 and 300 kg/m^2 s coincide within experimental uncertainty before and after the transition, which occurs at $0.2 \leqslant x \leqslant 0.3$; the data for 500 kg/m^2 s are only slightly higher and terminate at $x = 0.35$. The uncertainty is introduced by the data for

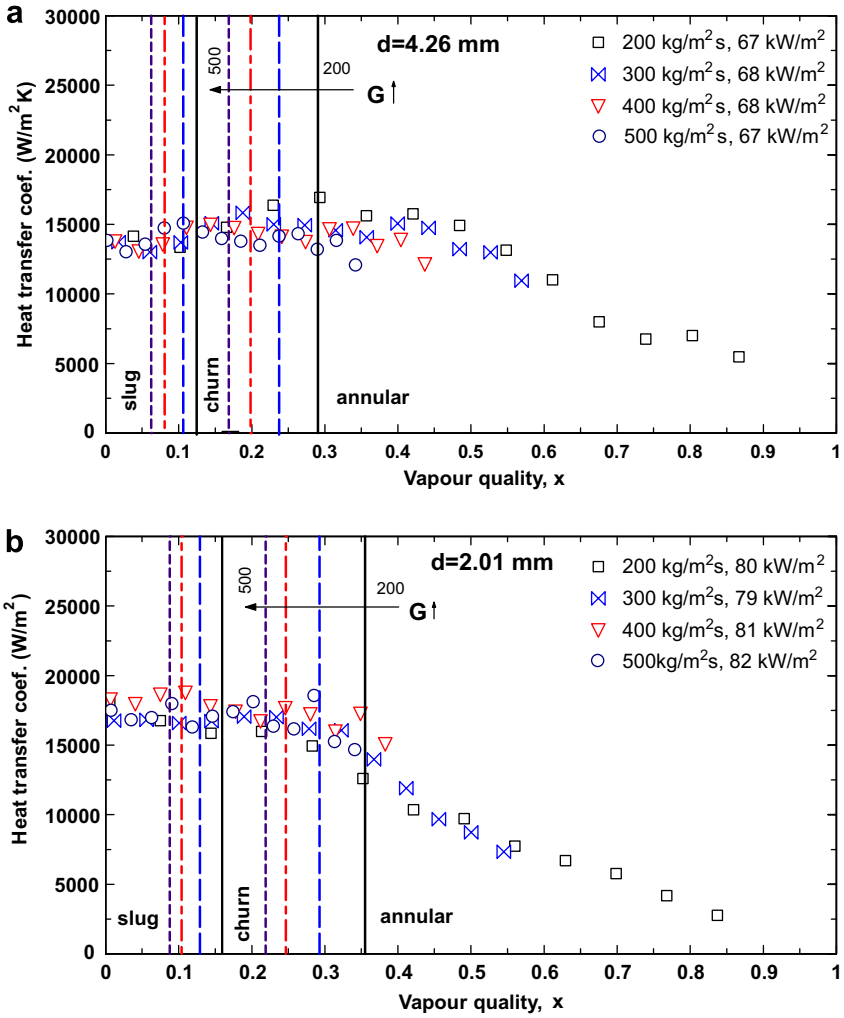

Fig. 4. Local heat transfer coefficient as a function of vapour quality for different mass flux, $P = 8$ bar: (a) $d = 4.26$ mm, nominal $q = 68$ kW/m^2 (b) $d = 2.01$ mm, nominal $q = 80$ kW/m^2.

400 kg/m^2 s, which may indicate transition at a higher value of $x \sim 0.36$ near the churn-annular boundary. If this is confirmed, the trend is in the opposite sense to that in the 4.26 mm tube. Further experiments are required to resolve the issue, using longer heated lengths to achieve larger exit qualities, subject to any limitations imposed by pressure drop.

The observed characteristics of the heat transfer coefficients at low quality are similar to those conventionally interpreted as evidence that flow boiling in large tubes is dominated by nucleate boiling: the coefficients increase with increasing heat flux and pressure but are insensitive to quality and mass flux. However, the three-zone evaporation model proposed by Thome et al. [1] suggests that, for small passages, the same behaviour can be explained if transient evaporation of the thin liquid film surrounding elongated bubbles, without nucleate boiling contribution, is the dominant heat transfer mechanism. This is not altogether surprising, because both mechanisms involve the cyclic creation and evaporation of thin liquid films which may involve small-scale dryout. This is on smaller length- and time-scales than the partial dryout that has been proposed as the probable explanation for the decreases in heat transfer with increasing quality observed in this study.

5. Comparison with some recent correlations and three-zone evaporation model

The heat transfer results were compared with some recent correlations and the three-zone evaporation model. The results and comments are presented below. The experimental data in the region of decreasing heat transfer coefficient with increasing quality are not included in the comparisons shown in Figs. 5–7. This is because the region is attributed to the intermittent dryout, which was not considered in the development of the correlations. The model considered a different form of intermittent dryout.

5.1. The 2004 Kandlikar [26] correlation

The comparison of the Kandlikar [26] correlation with the experimental results is depicted in Fig. 5. For both tubes at 8 bar pressure, the under-prediction exceeds 30% at low values of heat transfer coefficient. The prediction is better at higher heat transfer coefficient, although there is significant scatter. This may indicate that there is a systematic reason for deviations at low flow rates. The correlation is empirical, using a regression analysis of a large data bank. Different equations are proposed depending on the Reynolds number, which defines the flow regions. Therefore, the question of the uncertain boundary between turbulent flow and laminar flow in small tubes could affect the applicability of this correlation more than other correlations. There is no obvious diameter effect in this comparison, i.e. the disagreement is similar for both diameters studied. Also, there was no effect of pressure on the comparison, hence only typical prediction results at 8 bar system pressure are shown in Fig. 5.

5.2. The 2004 Zhang et al. [31] correlation

The comparison with the experimental results is presented in Fig. 6. For the 4.26 mm tube, the correlation predicts the results very well, i.e. within ±20% at a pressure of 8 bar. The results are under-predicted especially for the lower heat transfer coefficients by more than 30% at 12 bar pressure. In Fig. 6c and d, for the 2.01 mm tube, the correlation under-predicts the experimental results up to 30% for 8 bar and by more than 30% for the 12 bar pressure; the comparison is better at high heat transfer coefficient. There is bias in the predictions with changing system pressure and the 8 bar results are predicted better than those for 12 bar. In general, the correlation predicts the larger diameter tube experimental results better than the smaller tube. This could be due to the fact that the Zhang et al. [31] basically generalised Chen's [30] correla-

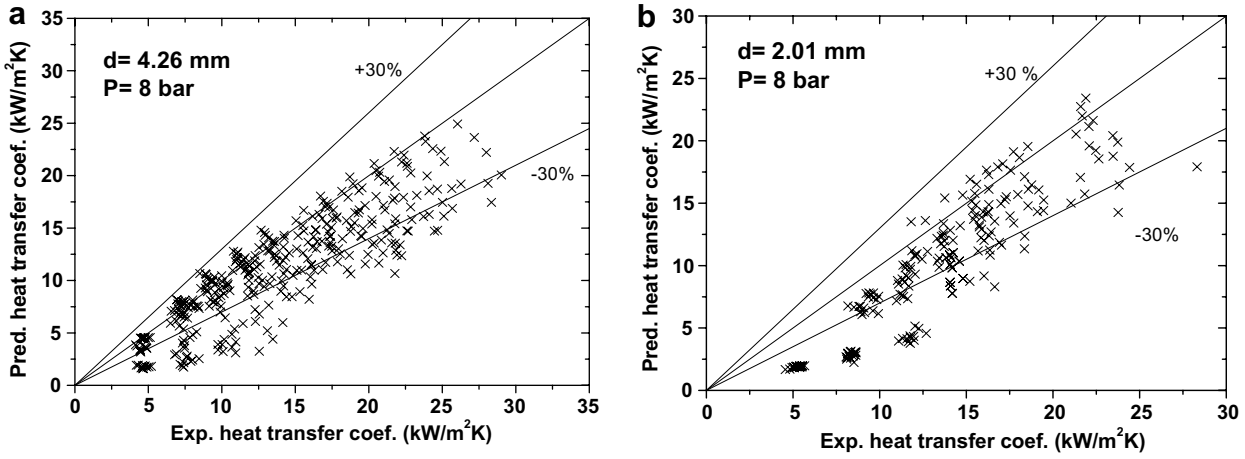

Fig. 5. Comparison between the local heat transfer coefficient and the corresponding experimental results predicted by Kandlikar and Balasubramanian [26] correlation.

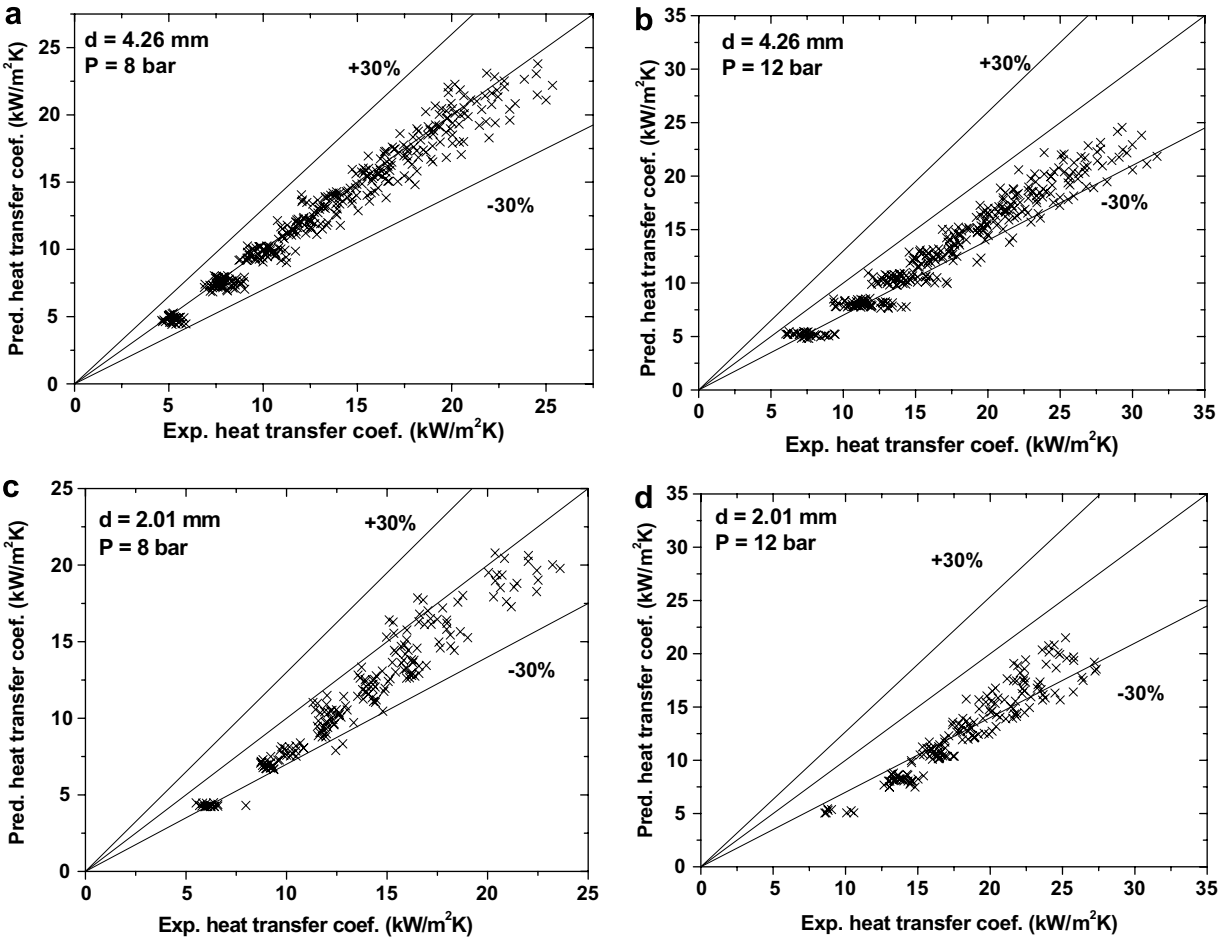

Fig. 6. Comparison between the local heat transfer coefficient and the corresponding experimental results predicted by Zhang et al. [31] correlation.

tion and hence based their work on the model proposed for conventional diameter heat transfer correlations.

5.3. The Thome et al. [1] three-zone evaporation model

The mechanistic three-zone evaporation model of Thome et al. [1], briefly described in Section 2, was developed assuming that slug flow is the prevailing flow pattern in small diameter tubes. Consequently, it should not be used outside this regime. The model does not include a prediction of its own range of validity by modelling the extinction of the liquid bridge between confined bubbles, so regime boundaries have been estimated based on [4]. The experimental data in the annular flow region and all data exhibiting the characteristics of partial dryout are omitted from the comparisons shown in Fig. 7. Strictly, data in the predicted churn flow regime should also be excluded, because instabilities at the liquid–vapour interface may enhance heat transfer by conduction through the liquid film, but they have been included here.

Fig. 7a includes a group of data points that are greatly under-estimated by the model. They are all associated with very low vapour qualities ($x \cong 0$ to 0.13), i.e. near the inlet to the test section. This serious disagreement may be attributed to the onset of nucleate boiling, i.e. exclusion from the model of bubble formation in the unconfined bubbly flow region. The model assumes all-liquid flow up to the inception of the confined bubbles at $x = 0$ and employs a laminar fully developed single-phase heat transfer correlation that gives heat transfer coefficients much lower than for unconfined bubbly flow. The examples in Thome et al. [1] always have a heat transfer coefficient that changes from a very low value at $x = 0$ to a large value at a small positive value of x, followed by a slight decrease with further increase in x, as seen in the following comparisons of the axial development of the experimental and predicted coefficients. These points at very low x have been omitted from the other plots in Fig. 7 as unrepresentative of fully-confined bubble flow.

The model consistently over-predicts the 4.26 mm data by 20–40% at a pressure of 8 bar. At a pressure of 12 bar, good agreement is achieved, i.e. within ±30%; there is a tendency to over-predict at higher values of the heat transfer coefficient. For the 2.01 mm tube, the data are predicted within ±20% at 8 bar and are mostly under-predicted by up to 30% at 12 bar. The data are more scattered for the 2.01 mm tube than for the larger 4.26 mm tube. On the whole, the three-zone evaporation

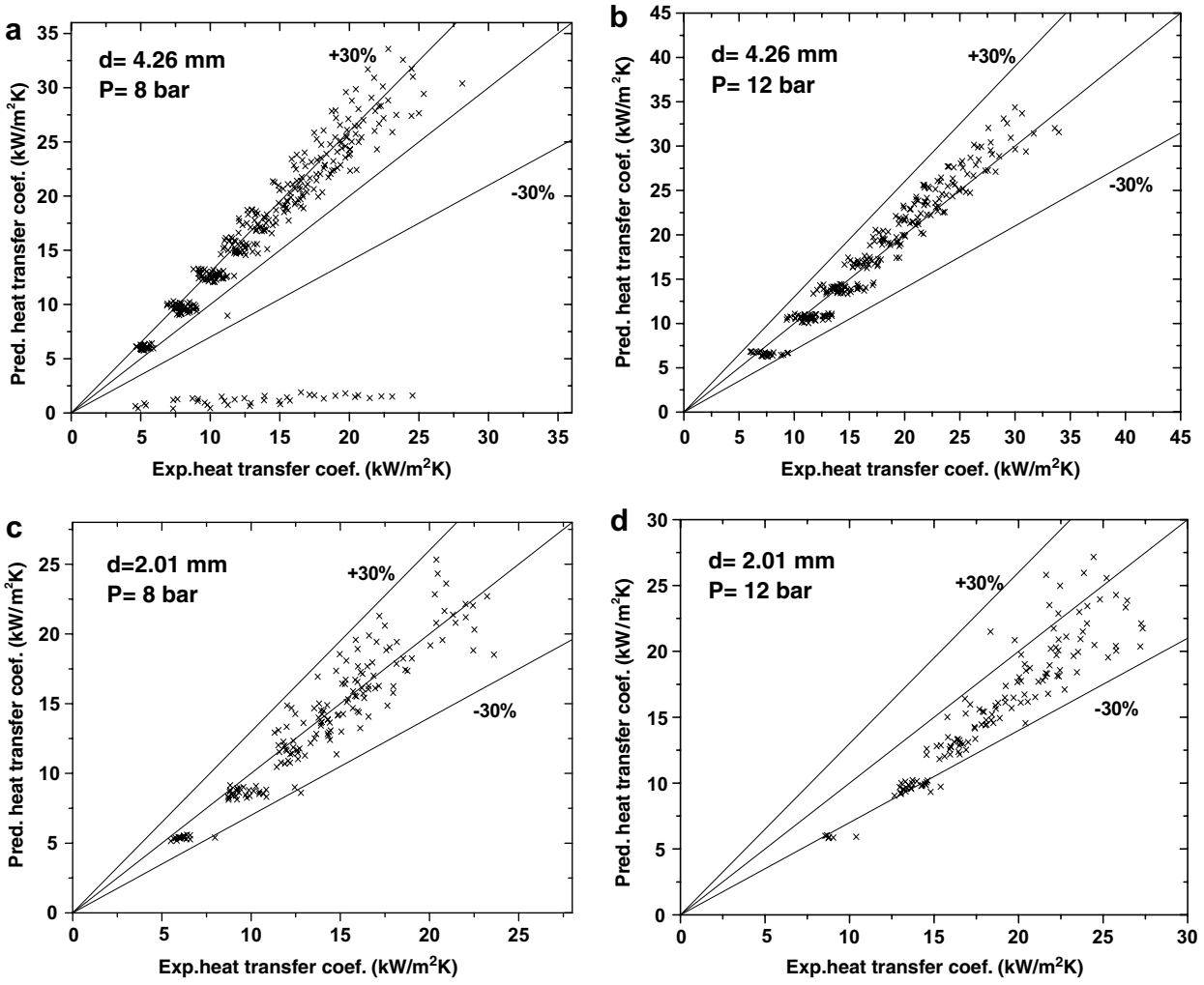

Fig. 7. Comparison between the local heat transfer coefficient predicted by the Thome et al. [1] model and the corresponding experimental results.

model predicts the experimental data at least as well as the rest of the correlations, which are based on large tube boiling correlations. This reasonably satisfactory global performance supports the proposition that a model that excludes nucleate boiling can nevertheless represent the "apparently nucleate boiling regime" but the bias in the predictions with changing tube diameter and system pressure suggests that the performance of the model should be examined more closely.

The comparisons between the model and the data are examined on a more detailed local basis in Figs. 8–10, plotting heat transfer coefficient against quality. These figures cover the full range of experimental qualities, because it appears that the model can make satisfactory predictions at qualities expected to be in the annular flow regime, up to the onset of partial dryout. The churn/annular transition boundary from Fig. 2 is also shown in Fig. 8 to indicate the extension of the model prediction in the annular regime. There may be some differences between the highly transient flow conditions within the heated test section and those observed in [4] in an adiabatic section following the test section, which require further investigation.

Fig. 8 shows the local heat transfer coefficient versus vapour quality for various heat fluxes at constant mass flux and at 8 bar pressure. The experimental values are always high at $x = 0$ and remain at approximately the same level up to the quality where partial dryout commences, with some fluctuations that are mostly within the bounds of experimental uncertainty. As seen in Fig. 8a, the model over-predicts the 4.26 mm tube data for the entire range, with the difference increasing with increasing heat flux. Heat transfer in the apparent conditions of partial dryout observed for $x > 0.55$ and $q \geqslant 97\ \mathrm{kW/m^2}$ is highly over-predicted by the model. The effect of heat flux on the experimental heat transfer coefficient gets smaller as the heat flux is increased; this is not well predicted by the model. As shown in Fig. 8b, for the 2.01 mm tube, the prediction is better at lower heat flux values, however the data is again over-predicted as the heat flux increases. The partial dryout observed for $x > 0.3$ and $q \geqslant 80\ \mathrm{kW/m^2}$ is also predicted poorly. The experimental heat transfer coefficient increases with heat flux for low to moderate heat flux values (20–80 $\mathrm{kW/m^2}$). At high heat flux values, $q > 80\ \mathrm{kW/m^2}$, the heat flux effect decreases and further increase in the heat

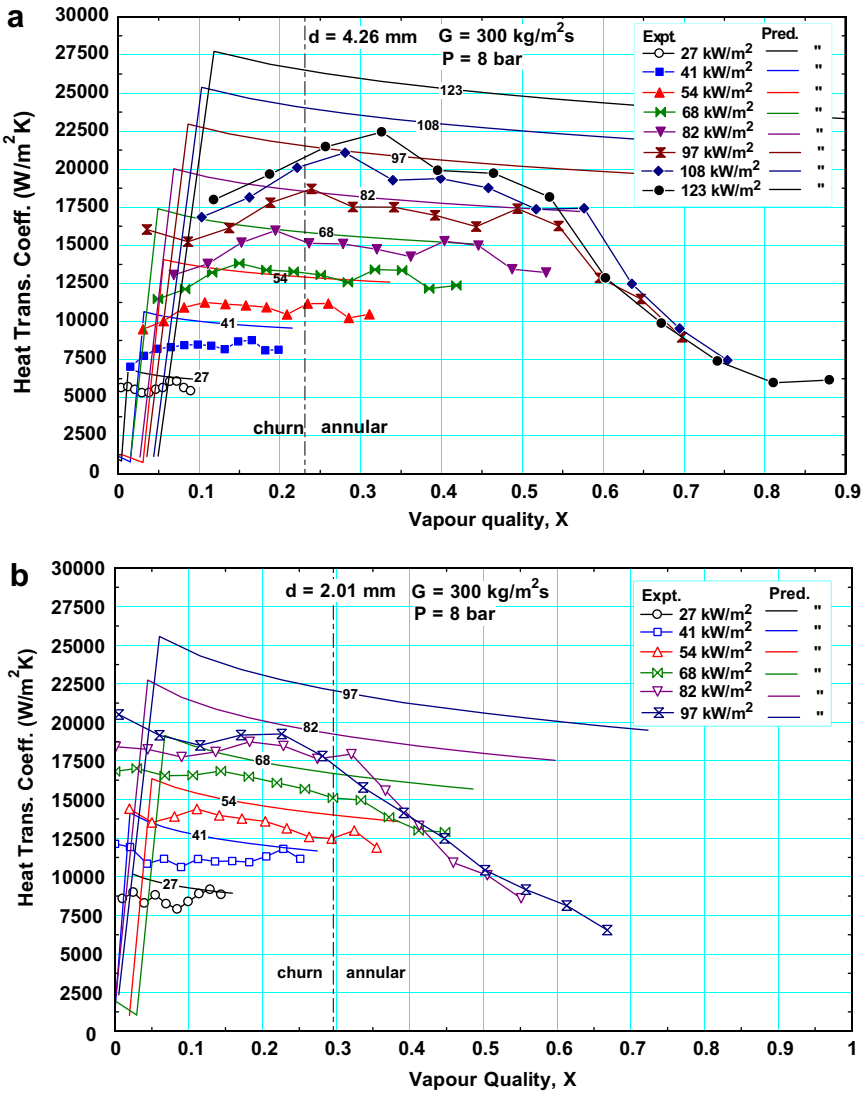

Fig. 8. Comparison of the local heat transfer coefficient versus vapour quality with the Thome et al. [1] model for various heat flux values and $P = 8$ bar: (a) $d = 4.26$ mm, (b) $d = 2.01$ mm.

flux produces a significant change in the characteristic of the curve and an opposite effect on the heat transfer coefficient for $x > 0.15$ until all heat flux lines merge. However, the predicted heat transfer coefficient increases with heat flux almost uniformly for all heat flux values, i.e. it continues increasing even at very high heat flux values, highly over-predicting the experimental data.

A comparison with the model for local heat transfer coefficient versus vapour quality for various combinations of mass flux and heat flux is depicted in Fig. 9 for the 4.26 mm and 2.01 mm tubes at a pressure of 8 bar and 12 bar. These figures are included to demonstrate the effect of mass flux and pressure on the prediction. Fig. 9a, for the 4.26 mm tube at pressure of 8 bar, shows that the model over-predicts the data with increasing mass flux and heat flux, as in Fig. 8a. However, in Fig. 9b at 12 bar, the larger diameter experimental results are predicted very well for $q \leqslant 60$ kW/m^2 and $G \leqslant 300$ kg/m^2 s. At higher values of heat and mass flux the model over-predicts the experiment results. In general, the prediction is highly improved as the pressure increases from 8 to 12 bar, because the model predicts the larger diameter tube data better at 12 bar than 8 bar. This indicates that the performance of the model is sensitive to system pressure. In Fig. 9c and d, the local heat transfer coefficient versus vapour quality is depicted for the 2.01 mm tube, at both pressures. Examination of Fig. 9c indicates a very good agreement with the experimental values in the range of quality $0.15 < x < 0.3$ for $G < 300$ kg/m^2 s and $q < 80$ kW/m^2. The experimental results are over-predicted outside the above quality range and the over-prediction increases as mass and heat flux values increase. Fig. 9d presents the same comparison for the same diameter but at a system pressure of 12 bar. The experimental data are slightly under-predicted at lower mass and heat flux ($G \leqslant 200$ kg/m^2 s, $q \leqslant 54$ k W/m^2). Above these values, the model tends to slightly over-predict

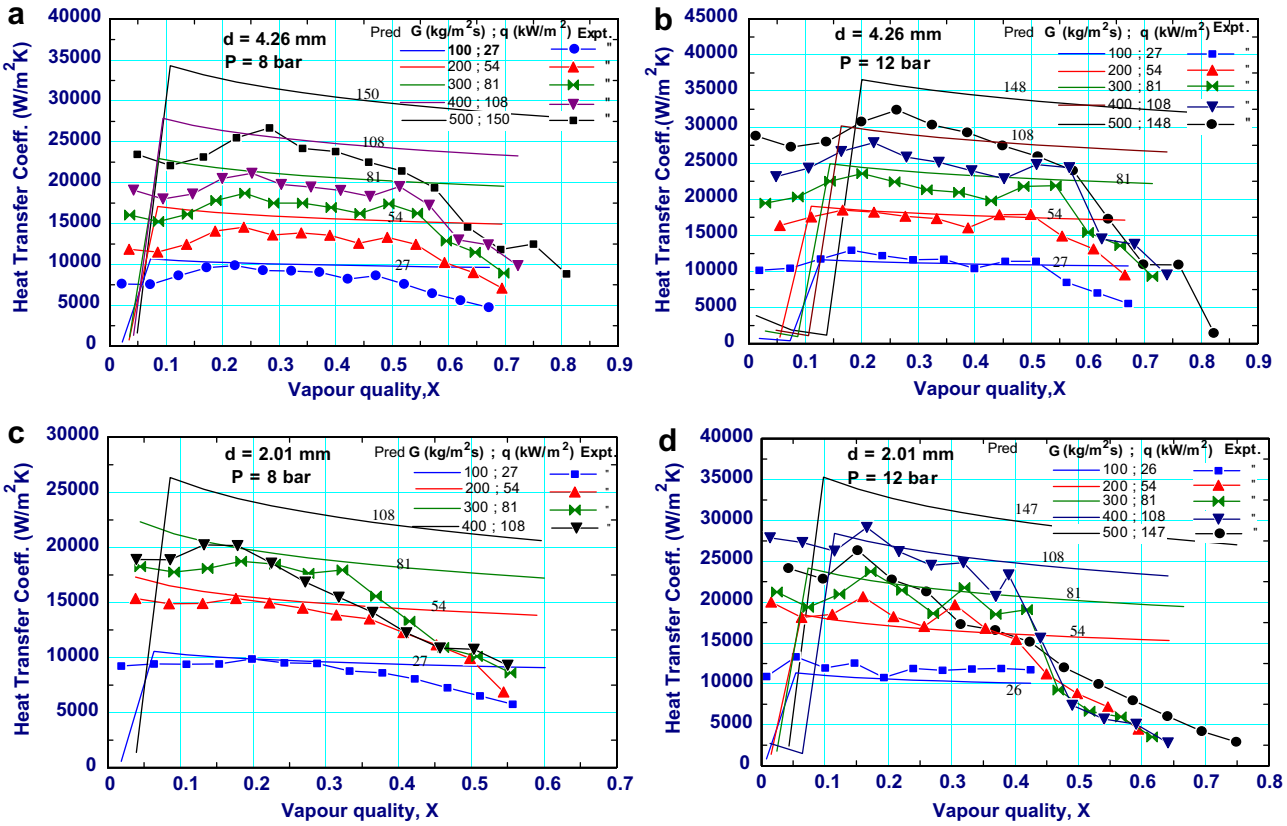

Fig. 9. Comparison of the local heat transfer coefficient versus vapour quality with the Thome et al. [1] model at various mass and heat flux values for: (a) $d = 4.26$ mm, $P = 8$ bar, (b) $d = 4.26$ mm, $P = 12$ bar, (c) $d = 2.01$ mm, $P = 8$ bar, (d) $d = 2.01$ mm, $P = 12$ bar.

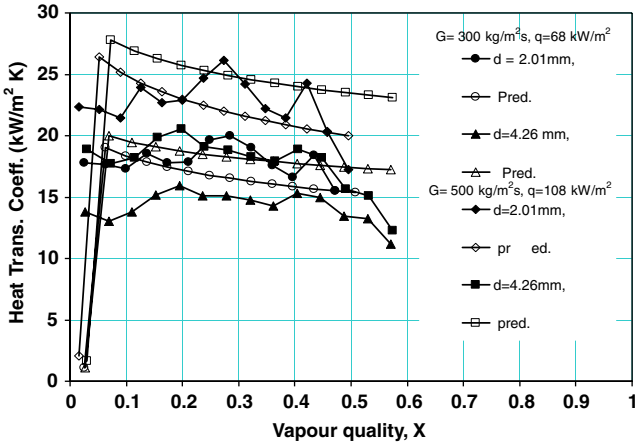

Fig. 10. Effect of diameter on local heat transfer coefficient in comparison with that predicted by the three-zone model at 8 bar pressure.

the data. A significant over-prediction is observed for the highest heat flux ($q = 147$ kW/m^2), for which the corresponding experimental results show a monotonic drop in heat transfer coefficient with quality, attributed to early dryout in the experiments.

In general, the predicted heat transfer coefficient tends to decrease slightly with vapour quality after a peak at around $x \sim 0.05$ to 0.1 for the entire range, for both diameters at both pressures, especially for high heat flux and mass flux values. The experimental results remain nearly constant until partial dryout occurs. The model includes a mechanism of periodic dryout under each confined bubble but the partial dryout region is highly over-predicted for all the data.

Fig. 10 presents the diameter effect as predicted by the model in comparison with the corresponding experimental result, at a system pressure of 8 bar. The experimental results show that the heat transfer coefficient decreases with increasing diameter. However, the model predicted an opposite effect of diameter on the heat transfer coefficient, i.e. the heat transfer coefficient for the larger diameter is higher than that of the smaller diameter. This was also observed by Dupont and Thome [34], who suggested that it could be due to the fact that the model is suited for smaller diameter tubes, as it is based on a flow pattern mostly observed in small diameters. The heat transfer coefficient versus heat flux in comparison with the model results is also shown in Fig. 11 for the 2.01 mm tube. Again, the experimental data in the region of decreasing heat transfer coefficient with increasing quality, indicative of partial dryout, are not included in this figure. The heat flux exponents obtained in the curve fitting are slightly higher for the model. However, both exponents are similar to a typical pool boiling correlation case.

The model prediction is highly sensitive to the initial and end film thickness of the confined bubble and the frequency

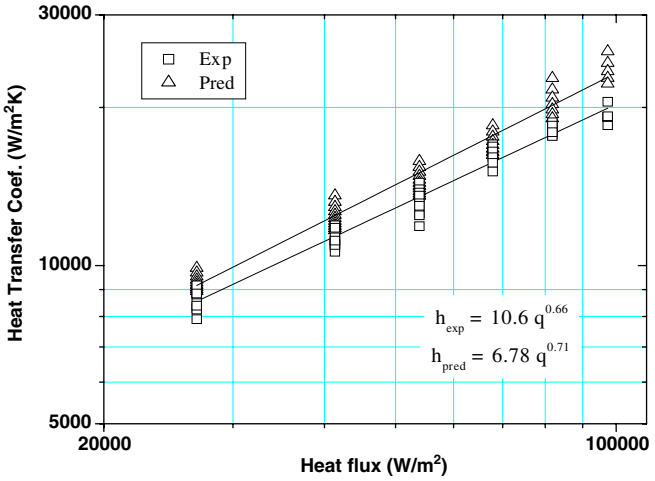

Fig. 11. Heat transfer coefficient versus heat flux of the experimental results and that predicted by three-zone model for $d = 2.01$ mm tube at $P = 8$ bar and $G = 300$ kg/m^2 s.

of bubble generation. The extent of the dryout zone is directly associated to the value of the end film thickness, which is one of the optimized parameters. Fig. 12 presents the heat transfer predictions by the model at various heat fluxes with modified parameters. When the critical end film thickness value for dryout (1.75 μm) is made approximately equal to the tube average roughness (1.82 μm), parameter C_{δ_0} is slightly changed to a value of 0.43 and the frequency of bubble generation (f) is 1.5 times that recommended by Dupont et al. [33], good predictions are obtained of the partial dryout case that occurred early at very low quality. This suggests that the distinction drawn earlier in this paper between cyclic dryout and more extensive partial dryout may require further consideration. The range of data is at present too small for definite conclusions but this example suggests that wall roughness may be a significant variable for flow boiling in small tubes. It has rarely been reported in past studies but it should be recorded in future measurements. Appropriate characterization of the roughness requires further investigation.

Based on the comparison above, features of the model that may require modification include the analytical determination of the bubble generation frequency, and the initial and end film thicknesses. The modifications by Thome et al. [1] of the Moriyama and Inoue [32] film thickness correlation for the prediction of the initial film thickness have eliminated the influence of bubble growth time. This modification results in an entirely different prediction of the behaviour for the condition of increasing bubble velocity in a tube of fixed radius, i.e. that the film thickness reaches maximum value and then decreases, which appears to be inconsistent with the available experimental evidence for steady flow. Also, the model assumes already formed elongated bubbles and does not include the inception of the elongated bubbles and their growth from departing bubbles, i.e. the initiation of the confined bubble regime at $x = 0$ needs to be revised. The model does not take account of the fluctuations in saturation temperature. This is a simplification which may or may not be valid in all circumstances, which must be examined further. Assessment of such variations may require a major extension of the model, if shown to be significant. The discrepancy in the pressure effect could be attributed to a limitation of the one-dimensional model, which does not solve the equation of motion for the liquid slug to allow for the variations in pressure. On the other hand, the high pressure gives higher vapour density that leads to lower vapour superficial velocity. As a result, pressure changes could cause a flow map shift, (i.e. a shift from elongated bubble regime) which affects the model applicability. At present, the model does not accommodate such variations. The model may also need to consider a cyclic

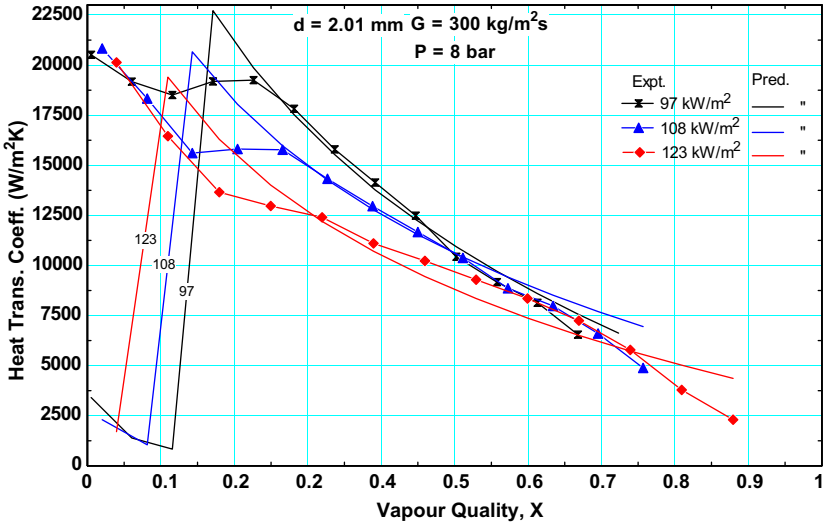

Fig. 12. Experimental results and predictions for continuous dry out cases when the critical film thickness value $\delta_{min} = 1.75$ μm, $C_{\delta 0} = 0.43$ and the frequency of bubble generation, f equals 1.5 times that recommended by Dupont et al. [33].

occurrence of nucleate boiling in thin film regions, as observed by Kenning and Yan [18], Wen et al. [19]. However, the model is at an early stage of development and may provide a good starting point for further work of this nature.

6. Conclusions

A global comparison of the existing correlations and a detailed analysis of the three-zone evaporation model were presented in this paper, based on experiments on R134a boiling in two sizes of tube over a range of pressures and mass fluxes. The experimental results for the 4.26 mm tube demonstrate that the heat transfer coefficient increases with heat flux and system pressure, but does not change with vapour quality when the quality was less than about 40–50%, for low heat flux. For the 2.01 mm tube, this boundary moves to 20–30% vapour quality. This behaviour at low quality is conventionally interpreted as evidence that nucleate boiling is the dominant heat transfer mechanism. For higher vapour qualities, the heat transfer coefficient becomes independent of heat flux and decreases with vapour quality. This could be caused by partial (intermittent) dryout.

A comparison of the present results with the existing correlations shows that the correlations cannot predict the heat transfer data satisfactorily. The state-of-the-art, three-zone evaporation model of Thome et al. [1] is based on convective heat transfer in the confined bubble regime, without any contribution from nucleate boiling. It is found that the model predicts experimental data that would be conventionally interpreted as nucleate boiling at least as well as any correlation, confirming the claims of its authors [1] that a model without a nucleate boiling contribution may provide a reasonably successful approximate prediction of the ''apparently nucleate boiling'' heat transfer regime.

The mechanistic model [1] should only be used in the slug flow regime for which it was developed. It was found that it gave satisfactory predictions extending into the annular flow regime, as defined by the studies in [4] based on quasi-equilibrium conditions in an adiabatic section following a boiling section. The relation between such observations and the highly transient conditions in boiling requires further investigation.

The model requires further development. It predicts that the diameter of the tube has opposite effect on the heat transfer coefficient as that indicated by the actual data. The pressure changes are seen to significantly affect the model prediction capability. Features of the model that may require modification include independent determination of the bubble generation frequency and the initial and end film thicknesses, the fluctuations in pressure and consequently in saturation temperature caused by the cyclic acceleration of the liquid slugs and the contribution from nucleate boiling before the position at which confined bubbles are formed.

The model does not predict satisfactorily the conditions of decreasing heat transfer coefficient that occurred in the 4.26 mm and 2.01 mm tubes at high quality and which are attributed to partial dryout. However, a satisfactory prediction was achieved for one example of partial dryout at high heat flux and low quality, by modifying the recommended values of the three disposable parameters in the model.

References

[1] J.R. Thome, V. Dupont, A.M. Jacobi, Heat transfer model for evaporation in microchannels, Part I: presentation of the model, Int. J. Heat Mass Transfer 47 (2004) 3375–3385.
[2] S.G. Kandlikar, W.J. Grande, Evolution of microchannel flow passages – thermohydraulic performance and fabrication technology, Heat Transfer Eng. 25 (1) (2003) 3–17.
[3] P.A. Kew, K. Cornwell, Correlations for the prediction of boiling heat transfer in small diameter channels, Appl. Thermal Eng. 17 (8–10) (1997) 705–715.
[4] L. Chen, Y.S. Tian, T.G. Karayiannis, The effect of tube diameter on vertical two-phase flow regimes in small tubes, Int. J. Heat Mass Transfer 49 (2006) 4220–4230.
[5] L. Chen, Flow patterns in upward two-phase flow in small diameter tubes, PhD thesis, Brunel University, UK, 2007.
[6] Y.Y. Yan, T. F Lin, Evaporation heat transfer and pressure drop of refrigerant R-134a in a small pipe, Int. J. Heat Mass Transfer 41 (1998) 4183–4194.
[7] B. Agostini, A. Bontemps, Vertical flow boiling of refrigerant R134a in small channels, Int. J. Heat Fluid Flow 26 (2) (2005) 296–306.
[8] B. Palm, Mini-and microchannel research in Sweden, in: Proceedings of 1st ASME International Conference in Microchannels and Minichannels, Rochester, New York, 2003, pp. 25–31.
[9] X. Huo, Experimental study of boiling heat transfer in small diameter tubes, PhD thesis, London South Bank University, London, UK, 2006.
[10] G.M. Lazarek, S.H. Black, Evaporative heat transfer, pressure drop and critical heat flux in a small vertical tube with R-113, Int. J. Heat Mass Transfer 25 (7) (1982) 945–960.
[11] M.W. Wambsganss, D.M. France, J.A. Jendraejczyk, T.N. Tran, Boiling heat transfer in a horizontal small-diameter tube, J. Heat Transfer 115 (1993) 963–972.
[12] T.N. Tran, M.W. Wambsganss, D.M. France, Small circular- and rectangular-channel boiling with two refrigerants, Int. J. Multiphase Flow 22 (3) (1996) 485–498.
[13] Z.Y. Bao, D.F. Fletcher, B.S. Haynes, Flow boiling heat transfer of Freon R11 and HCFC123 in narrow passages, Int. J. Heat Mass Transfer 43 (2000) 3347–3358.
[14] X. Huo, Y.S. Tian, T.G. Karayiannis, R134a Flow boiling heat transfer in small diameter tubes, Advances in Compact Heat Exchangers, R.T. Edwards, Inc., 2007, pp. 95–111 (Chapter 5).
[15] V.P. Carey, P. Tervo, K. Shullenberger, Partial dryout in enhanced evaporator tubes and its impact on heat transfer performance, SAE Tech. Paper (1992) 920551.
[16] Y. Yan, D.B.R. Kenning, Pressure and temperature fluctuations during boiling in narrow channel, Eurotherm 62: Heat Transfer Condensation Evaporation, Grenoble (1998) 107–1223.
[17] P.A. Kew, K. Cornwell, On pressure fluctuations during boiling in narrow channels, in: 2nd European Thermal-Science and 14th UIT National Heat Transfer Conference, Rome, 1996, pp. 1323–1327.
[18] D.B.R. Kenning, Y. Yan, Saturated flow boiling of water in a narrow channel: experimental investigation of local phenomena, IChemE Trans. A, Chem. Eng. Res. Design 79 (2001) 425–436.
[19] D.S. Wen, Y. Yan, D.B.R. Kenning, Saturated flow boiling of water in a narrow channel: time-averaged heat transfer coefficients and correlations, Appl. Thermal Eng. 24 (2004) 1207–1223.

[20] D. Brutin, L. Tadrist, Pressure drop and heat transfer analysis of flow boiling in a microchannel: influence of the inlet condition on two-phase flow stability, Int. J. Heat Mass Transfer 47 (2004) 2365–2377.
[21] L. Zhang, K.E. Goodson, T.W. Kenny, Silicon Microchannel Heat Sinks, Theories and Phenomena, Springer, Berlin, 2004 (Chapters 5–7).
[22] L. Zhang, E.N. Wang, K.E. Goodson, T.W. Kenny, Phase change phenomena in silicon microchannels, Int. J. Heat Mass Transfer 48 (2005) 1572–1582.
[23] D.S. Wen, D.B.R. Kenning, Y. Yan, Flow boiling of water in a narrow vertical channel at low mass flux: observations of local phenomena, in: Proceedings of the 12th International Heat Transfer Conference, Grenoble, vol. 3, 2002, pp. 773–778.
[24] D.B.R. Kenning, D.S. Wen, K.S. Das, S.K. Wilson, Confined growth of a vapour bubble in a capillary tube at initially uniform superheat: experiments and modelling, Int. J. Heat Mass Transfer 49 (2006) 4653–4671.
[25] K.E. Gungor, R.H.S. Winterton, A general correlation for flow boiling in tubes and annuli, Int. J. Heat Mass Transfer 29 (1986) 351–358.
[26] S.G. Kandlikar, P. Balasubramanian, An extension of the flow boiling correlation to transition, laminar, and deep laminar flows in minichannels and microchannels, Heat Transfer Eng. 25 (3) (2004) 86–93.
[27] S.G. Kandlikar, A general correlation for saturated two-phase flow boiling heat transfer inside horizontal and vertical tubes, J. Heat Transfer 112 (1990) 219–228.
[28] V. Gnielinski, New equations for heat and mass transfer in turbulent pipe and channel flow, Int. Chem. Eng. 16 (1976) 359–368.
[29] B.S. Petukhov, V.N. Popov, Theoretical calculation of heat exchange in turbulent flow in tubes of an incompressible fluid with variable physical properties, Teplofiz. Vysok. Temperature (High Temperature Heat Phys.) 1 (1) (1963) 69–83.
[30] J.C. Chen, A correlation for boiling heat transfer to saturated fluids in convective flow, I&EC Process Des. 5 (1966) 322–329.
[31] W. Zhang, T. Hibiki, K. Mishima, Correlation for flow boiling heat transfer in mini-channels, Int. J. Heat Mass Transfer 47 (2004) 5749–5763.
[32] K. Moriyama, A. Inoue, Thickness of the liquid film formed by a growing bubble in a narrow gap between two horizontal plates, J. Heat Transfer 118 (1996) 132–139.
[33] V. Dupont, J.R. Thome, A.M. Jacobi, Heat transfer model for evaporation in microchannels, Part II: comparison with the database, Int. J. Heat Mass Transfer 47 (2004) 3387–3401.
[34] V. Dupont, J.R. Thome, Evaporation in microchannels: influence of the channel diameter on heat transfer, J. Microfluid. Nanofluid. (2004) 119–125.